scientific reports

Check for updates

OPEN

# Biosynthesis of CuO nanoparticles using aqueous extract of herbal tea (*Stachys Lavandulifolia*) flowers and evaluation of its catalytic activity

Hojat Veisi[1]✉, Bikash Karmakar[2]✉, Taiebeh Tamoradi[1], Saba Hemmati[1], Malak Hekmati[3] & Mona Hamelian[1]

**Plant derived biogenic synthesis of nanoparticles (NP) has been the recent trend in material science as featured sustainable catalysts. A great deal of the current nanocatalytic research has been oriented on the bio-inspired green catalysts based on their wide applicability. In this context, CuO NPs are synthesized following a green approach using an herbal tea *(Stachys Lavandulifolia)* flower extract. The phytochemicals contained in it were used asthe internal reductant without applying harsh chemicals or strong heat. The derived nanoparticles also got stabilized by the biomolecular capping. The as-synthesized CuO NPs was characterized over FT-IR, FE-SEM, EDS, TEM, XRD, TGA and UV–Vis spectroscopy. These NPs were exploited as a competent catalyst in the aryl and heteroaryl C–heteroatom (N, O, S) cross coupling reactions affording outstanding yields. The nanocatalyst was isolated and recycled in 8 consecutive runs with reproducible catalytic activity. Rigidity of the CuO/*S. Lavandulifolia* nanocomposite was further justified by leaching test and heterogeneity test.**

In the last few years designing of nanoparticles with tunable morphology with controlled shape, dimension and orderedness has been a significant area of concern in material science. A high degree of research has been carried out in view of their tremendous applications in diverse fields like chemo and biosensing, medicinal therapeutics, particularly as antimicrobial, antibacterial, anticancer agents, drug delivery systems, energy saving devices, optics, optoelectronics, electrochemistry andcatalysis[1–9]. The nanometric dimension, unique shape and large surface area has been beneficial in their distinctive catalytic properties. Further surface modifications over these materials by post-functionalization approach introduces unique physical properties[10–13]. A number of chemical and physical approaches are being encroached for the fabrication of NPs following top down or bottom up approach[14,15]. Nevertheless, most of the synthetic methods involve harsh conditions like strong reducing agents, elevated temperatures, high pressure and generates hazardous by-products *in-situ* which is deterrent for green protocol[16,17]. In some cases, the methodologies are tedious and expensive too. Thereby, the exploitation of biometric, clean, and eco-friendly procedures for the synthesis of NPs has increasing demand in view of green nanotechnology[18–23]. Notably, nature has provided a great resource in this regard and can be considered as an eco-bio-laboratory. Natural resources, especially different plant derived extracts like leaves, flowers, barks, fruit juices, fruit peels etc. are advantageous over physical and chemical methods. They are easily available, abundant, cheap, environmentally benign, and most importantly contains numerous phytochemicals (e.g., polyphenols, mild acids, alkaloids, terpenoids, flavonoids etc.) that are mild and very effective in the transformation of metal precursors towards the NPs. Moreover, the biogenic NPs are internally stabilized by the biomolecules as capping agents. They also protect the NPs from self-aggregation. In the last few years quite a number of methods have been reported on the biogenic synthesis of noble metal NP[24–31]. These very advantages have encouraged us to prefer the green biometric approach in the preparation of CuO NPs over an indigenous herbal tea flowers (*Stachys lavandulifolia*) extract (Fig. 1). The plant is grown abundantly in the hills of Kermanshah, Zagros area

[1]Department of Chemistry, Payame Noor University, Tehran, Iran. [2]Department of Chemistry, Gobardanga Hindu College, 24-Parganas (North), India. [3]Department of Organic Chemistry, Faculty of Pharmaceutical Chemistry, Tehran Medical Sciences, Islamic Azad University, Tehran, Iran. ✉email: hojatveisi@yahoo.com; bikashkarm@gmail.com

**Figure 1.** Image of *Stachys lavandulifolia* genum.

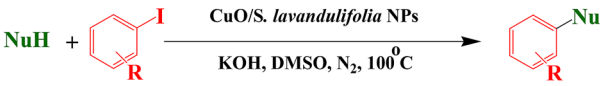


**Nu = ArNH, ArO, ArS**

**R = EDG, EWG**

**Scheme 1.** C–heteroatom cross coupling reactions over CuO NPs.

of western Iran and is popularly known as mountain tea (*Chay-e-Kouhi*). The herb is basically used as traditional medicinal plant in Iran[32].

Transition metals (Pd, Pt, Au, Ag, Rh, Ir etc.) are known to be distinctive catalysts in their ability to form bonds regardless their cost and sensitivity[33–39]. In this context, Cu has its unique features in terms of its abundance, cost effectiveness, eco-benevolence and stability. The CuO NP has wide implications in the field of thermal conductance, gas sensing, magnetic recording media, solar cell applications and pharmacology[40–44]. In modern trend of research, "NP catalyzed Organic Synthesis Enhancement" (NOSE) approach has been well-admired[30,45]. In promotion of NOSE chemistry, we herein report a green and expedient protocol for the C–heteroatom (N, O, and S) cross coupling catalyzed over biogenic CuO NP (Scheme 1)[46]. These products especially the heterocyclic coupled ones have extremely important biological, pharmaceutical and material values[47–50].

Earlier, a number of research groups like Weingarten, Chan-Lam, Buchwald, Taillefer, Ma, Punniyamurthy have reported the Cu catalyzed carbon-heteroatom cross coupling reactions[51–58]. However, most of them used different ligand based homogeneous catalysts or heterogeneous catalysts being generated by using toxic and strong reducing agents. The reusability of catalysts and greenness has been an important issue therein. In comparison, our protocol is free from the toxic reducing agents and external stabilizers, involves low cost green procedure for the biogenesis of CuO NPs and the material being used in the efficient, ligand free synthesis of C–N/O/S coupled products at short reaction time, making the overall procedure industrially and sustainably viable.

## Experimental

**Synthesis of herbal tea extract.** The fresh *S. lavandulifolia* (10 g) flowers were cleaned, dried and spread over 100 mL Milli-Q water and warmed at 60 °C for 15 min. The extract was filtered using Whatmann No. 1 filter paper and centrifuged on at 6000 rpm for 5 min to discard the probable aggregations. Finally, the clear extract was preserved at 4 °C for further use.

**Biogenic synthesis of CuO NPs over plant extract.** In order to prepare the CuO NPs, 10 mL of the extract was mixed to 100 mL 1 mM $Cu(OAc)_2$ solution and the mixture was heated at 80 °C for 100 min. The formation of NP was confirmed by change in color to dark brown, an outcome of surface plasmon resonance excitation. The resulting sediments were rinsed thrice with deionized water, chloroform and ethanol successively and finally dried in air for 48 h.

**Typical procedure for C–heteroatom cross-coupling reactions over CuO/*S. lavandulifolia* NPs.** A mixture of N/O/S nucleophile (1 mmol), aryl halide (1.1 mmol), KOH (1.5 mmol) and 3 mol % CuO/*S. lavandulifolia* NPs in dry DMSO (3 mL) was heated at 100 °C at inert conditions. After completion (by

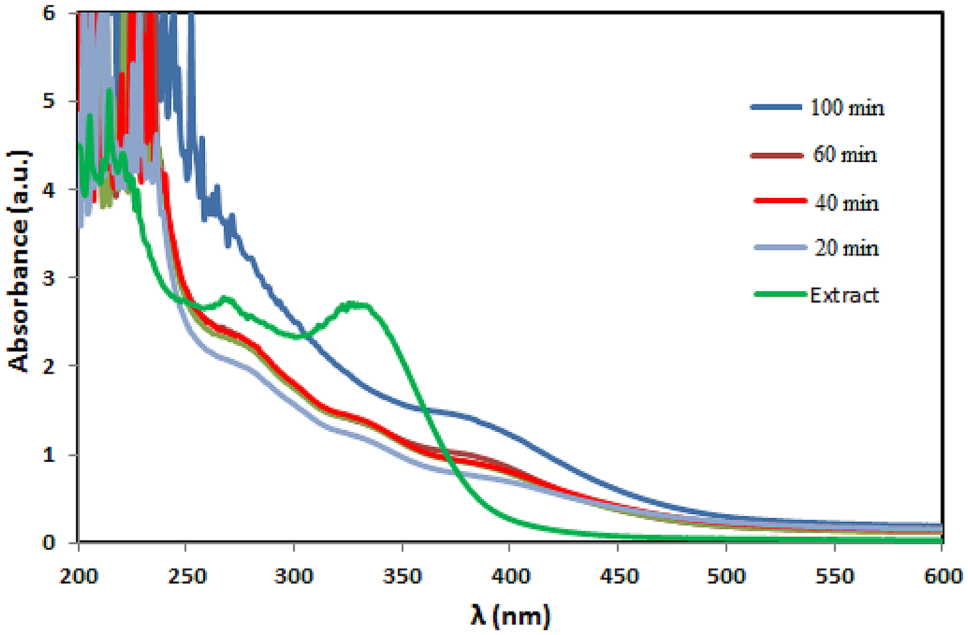


**Figure 2.** UV–Vis spectrum of biogenic CuO NPs using *S. lavandulifolia* extract.

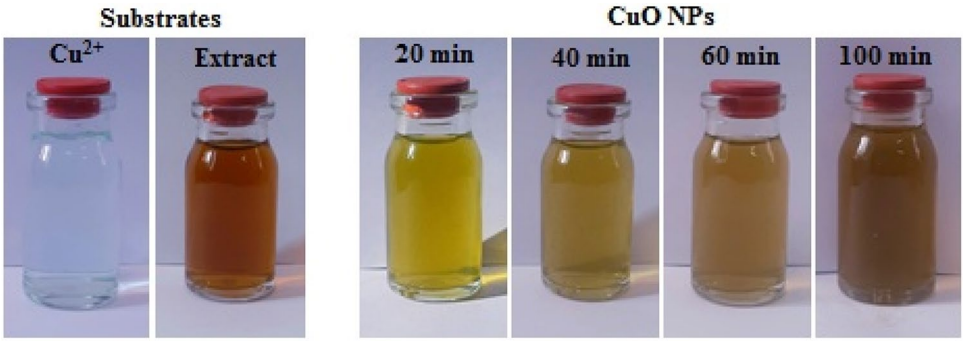


**Figure 3.** Visible detection of the biosynthesis of CuO NPs.

TLC), the reaction was worked up by adding into water (3 mL) and the organic layer was extracted with EtOAc. It was then washed with brine solution (10 mL), dried over $Na_2SO_4$ and concentrated. The crude product was finally purified over silica gel column chromatography using EtOAc/hexane mixture as eluent.

## Results and discussion

CuO NPs were synthesized following a green synthetic approach by *Stachys lavandulifolia* herb (Fig. 1). The primary phytochemical screening of the extract showed the existence of flavonoinds, triterpenoids, steroids, cardenolides, and alkaloids. During in *situ* synthesis, these phytochemicals play as the reducing agent to convert $Cu^{2+}$ ions to Cu NPs and simultaneously act as effective capping agent to prevent the NPs agglomerations. In the resulting procedure Cu(0) gets aerially oxidized to CuO NPs by heating. The as synthesized NPs were analytically characterized over different techniques like UV–Vis and FT-IR spectroscopy, FESEM, EDX, TEM, XRD and TGA.

UV–Vis spectroscopy is a potential measure for the identification of CuO NPs. The spectrum recorded at different time intervals of the reaction are presented in Fig. 2. After 100 min, the reaction was ended with the formation of CuO NPs, which was confirmed by the characteristic surface plasmon absorbance (sky blue line) at 400 nm. The variation in color of the reaction aliquots towards the formation of CuO NPs are depicted in Fig. 3.

FT-IR analysis was carried out to detect the probable biomolecules present in the aqueous extract of *S. lavandulifolia* responsible for the green synthesis of CuO NPs. Figure 4 shows the FT-IR spectrum of the plant extract and CuO/*S. lavandulifolia* nanocomposite. The spectrum of the plant extract represents several bands ranging from 3100 to 3385 $cm^{-1}$ which are attributed to free hydroxyl groups and their intra/intermolecular H-bonds of polyphenolic compounds[59,60]. The sharp peaks appeared at 2922, 1618 and 1398 $cm^{-1}$ were related to saturated hydrocarbons ($C_{Sp3}$-H) and C=O and C=C aromatic stretching frequencies respectively. The spectrum corresponding to CuO NPs is presented in Fig. 4b. The observed bands are due to lattice vibrational modes

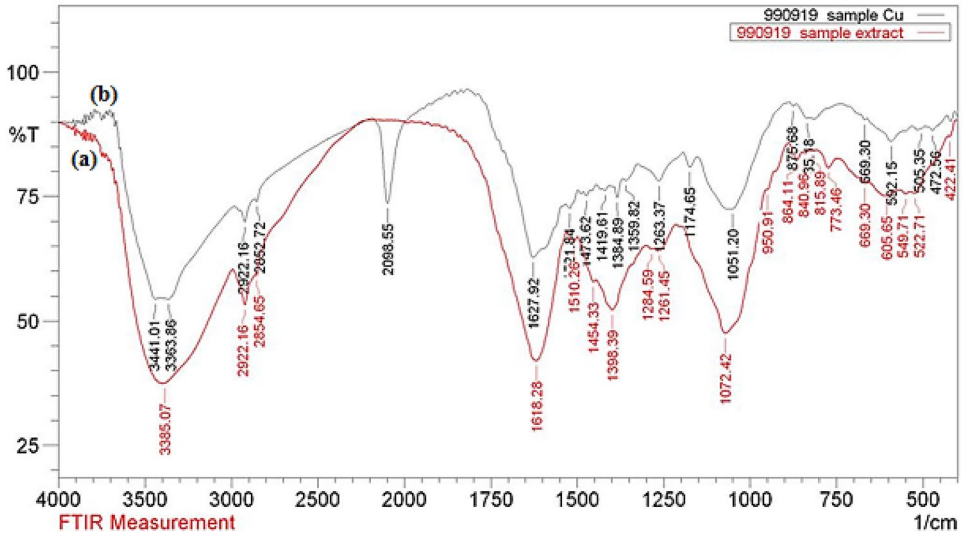


**Figure 4.** FT-IR spectrum of aqueous extract of *Stachys lavandulifolia* (**a**), and green synthesized CuO NPs (**b**).

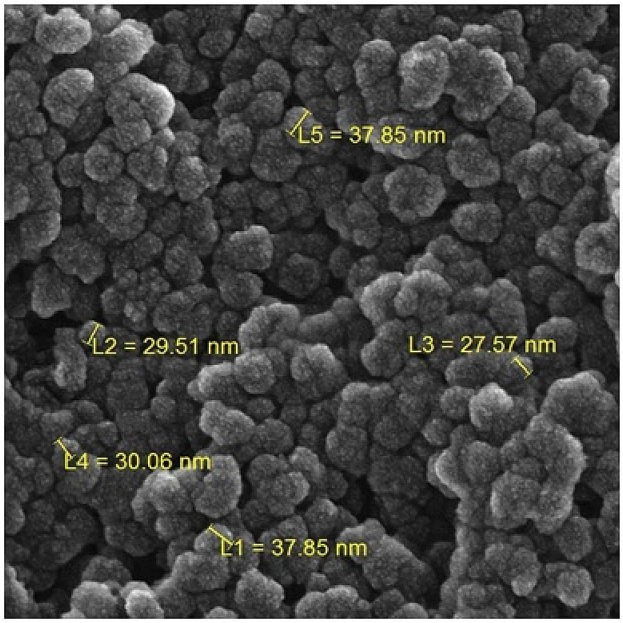


**Figure 5.** FE-SEM study of biogenic CuO NPs.

representing the functional groups of biomolecules supported NPs. The broad band around 3400 $cm^{-1}$ was related to OH stretching frequency. The peak at 1473 $cm^{-1}$ and 1627 $cm^{-1}$ was assigned to the bending vibrations of $sp^2$-bonds of aromatic moieties and carbonyl stretching frequencies respectively. Different organic functional moieties like amides, ethers and other aliphatic groups surrounded over CuO NP are specified by the peaks observed at 1263, 1174 and 1051 $cm^{-1}$. The phonon bands seen at 505 and ~ 592 $cm^{-1}$ represents the stretching vibration of Cu–O bond in monoclinic CuO[24].

The FE-SEM image presented in Fig. 5 indicates the defined spherical morphology of the prepared CuO NPs. All CuO NPs have the mean particles size of 20–35 nm. It is observed that biogenic synthesis of CuO NPs results comparably small spherical particles with uniform dimension. Clearly, small nuclear particles are self-aggregated and orient themselves to form larger spheres. Composition of the as-synthesized material being analyzed through EDX study, is observed in Fig. 6. The spectrum shows C, N, Cu and O peaks. The presence of oxygen in the profile demonstrates the oxidation of prepared $Cu^0$ NPs occurred upon exposure to air. The C and N atoms correspond to the phytochemicals from plant extract being bonded to CuO NPs.

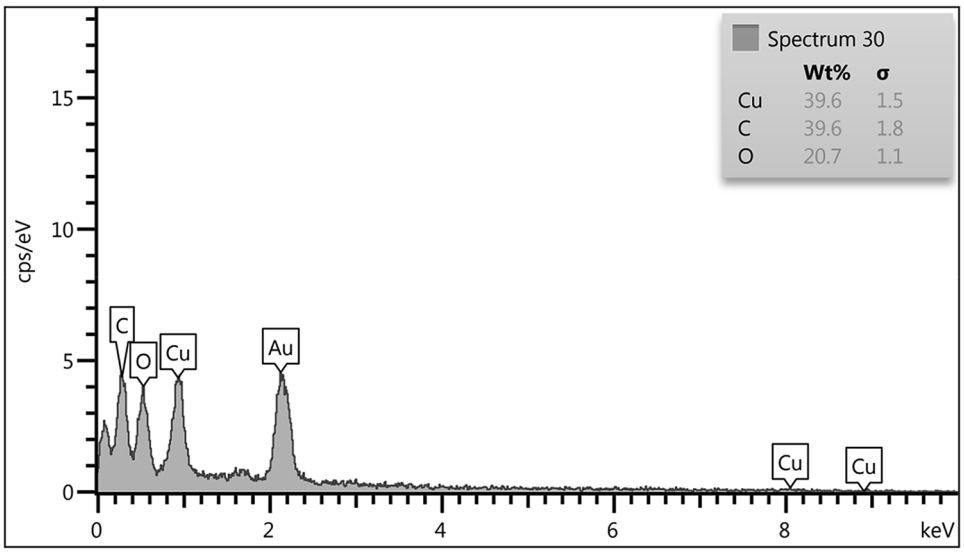


**Figure 6.** EDX analysis of biogenic CuO NPs.

The TEM analysis provides detailed morphological insights regarding the shape and dimension of CuO NPs. Figure 7 exhibits that the NPs are synthesized with moderately good monodispersity, having almost spherical structures ranging from 15 to 25 nm without any agglomeration.

Crystallinity of the green prepared CuO NPs was ascertained by XRD study (Fig. 8). The observed diffraction sharp peaks position at $2\theta = (32.59°, 35.61°, 38.78°, 48.82°, 53.54°, 58.37°, 61.60°, 66.31°, 68.15°, 72.46°$ and $75.30°$ were assigned to (1 1 0), (− 1 1 1), (1 1 1), (− 2 0 2), (0 2 0), (2 0 2), (− 1 1 3), (− 3 11), (2 2 0), (3 1 1) and (− 2 2 2) are highly consistent with JCPDS standard no. 01-080-0076 of CuO NPs with a monoclinic phase[61].

The level of % purity of CuO NPs in the composite was approximately 76.1 wt% as confirmed from the TGA, presented in Fig. 9. The mass decay observed in the region of < 200 °C was due to physisorbed water and organic polyphenolic bodies. Almost 17.12 wt % decrease in weight was reported at 200–600 °C resulting from the degradation of organic species. As the decomposition starts after 130 °C, the catalyst remains active at our reaction condition (100 °C) without any deformations.

There have been several reports for the bio-inspired synthesis of nanomaterials where polyphenolic compounds function as green reductants[62]. Incidentally, *Stachys lavandulifolia* is known to have a rich source of polyphenolic and flavonoidic compounds[63,64]. These phytochemicals play the role of reductant to Cu NPs. Scheme 2 represents a possible pathway towards the biogenesis of CuO NPs. Initially, the plant extract combined with the metal salt solution results in a polyphenolic complex with the $Cu^{2+}$ ion and consummated reduction generates $Cu^0$ NPs. The metallic Cu atoms further get oxidized over atmospheric oxygen forming stable CuO NP. Nucleation of the synthesized CuO NP promotes the growth towards isolable materials.

Once having the structural affirmation of biogenic CuO NPs by rigorous instrumentation, the catalytic performance of these NPs was assessed in the carbon-heteroatom cross coupling reactions. However, prior to general studies, optimization of the reaction conditions seemed quite significant and thereby a model reaction of iodobenzene with three N, O and S nucleophiles, viz., indole, phenol and thiophenol was screened with an array of experiments applying diverse conditions like catalyst load, solvent, base and temperature. The results have been documented in Table 1. While carrying out the C–N coupling reactions of indole, it failed in the absence of catalyst and the additive base (Table 1, entry 8, 10) indicating their importance. Among the different bases used, KOH was found to be most effective resulting highest yield at 100 °C (Table 1, entry 8). We also screened the reaction in different solvents like EtOH, toluene, DMF, DMSO, $CH_2Cl_2$, $CH_3CN$ (entry 1–8) when the best result was achieved in DMSO in shortest interval. Again, 3 mol% catalyst load was found optimum to have the best catalytic results (Table 1, entry 8). We examined the reaction at different temperature too. However, at lower temperature conditions it was not much successful and we continued the reactions at 100 °C (Table 1, entry 15, 16). After the fruitful experimentation for the best reaction conditions with N nucleophile (indole), we continued the same with other nucleophiles like O (phenol) and S (thiophenol) and delighted to have excellent outcomes at shorter reaction times (Table 1, entry 17, 18). Therefore, the best results for the Ar–C–N/O/S coupling were obtained by heating a mixture of 1.0 mmol iodobenzene, 1.1 mmol nucleophile and 1.5 mmol KOH in DMSO over 3 mol% CuO/*S. lavandulifolia* NP as catalyst.

After having the stabilized conditions, it was the turn to prove the generality of them over a wide range of heteroatom nucleophiles reacting with diverse aryl iodides to furnish a library of cross coupled products. The results have been shown in Table 2. Different aryl and heteroaryl N-nucleophiles like indole, imidazole and aniline reacts with high compatibility with diverse aryl iodides having electron accepting ($NO_2$) and electron releasing functional groups (Cl, $CH_3$, $OCH_3$), affording outstanding yields (Table 2, entry 1–15). Notably, aniline reacted with the aryl iodides at a faster rate than indole or imidazoles (Table 2, entry 7–12). The same reaction trend is followed with O-nucleophiles like substituted phenol derivatives and S-nucleophiles like substituted thiophenol derivatives with different aryl iodides. Interestingly, here also the corresponding nucleophiles reacted excellently

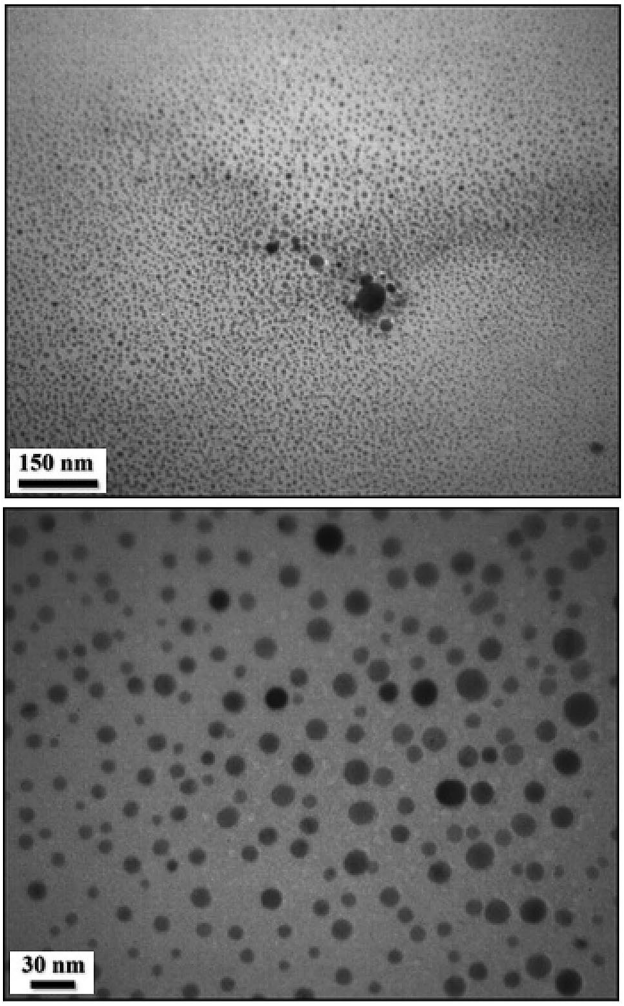


**Figure 7.** TEM images of biogenic CuO NPs.

to manage very good yields irrespective of the substitutions. All the coupled products were authenticated by literature studies and also corroborated by spectroscopic analysis.

While concerning about the mechanism, it is anticipated that the reaction pathway involves oxidative addition and subsequently reductive elimination. At the outset, Aryl halide molecule binds to the surface of biogenic CuO NPs. At intermediate stage, the nucleophile reacts with KOH to generate the potassio salt of them which further substitutes the halide ion bonded to catalyst surface. The Aryl group and nucleophile finally adds up over the catalyst and gets eliminated as coupled product leaving behind the active catalyst.

**Study of reusability and heterogeneity.** While concerning about the green reaction protocol, reusability of catalyst is an imperative aspect. In order of that, a probe reaction (entry 1, Table 2) with twice batch size was carried out under optimized conditions. After completion, the catalyst was retrieved on centrifuger, washed with EtOH, dried and recycled. Interestingly, we could use it for 8 successive runs without discernible change in its activity (Fig. 10). The morphology of the isolated catalyst was checked after 7th run of the reaction and found to remain intact as confirmed from FESEM and TEM analysis (Fig. 11). The catalyst was robust enough and no leaching was detected even after 7th run, as determined by ICP-OES. Furthermore, a hot filtration test was carried out to determine the heterogeneity of the catalyst, for the same above reaction. The reaction was paused after 5 h of fresh run and the catalyst was separated out of the reaction and continued further. Significantly, no additional increment in yield was detected, justifying true heterogeneity.

## Conclusion

In summary, we illustrate a bio-inspired green synthesis of CuO NPs followed by its catalytic applications. An herbal tea, *Stachys lavandulifolia* extract has been used as the plant source for biogenesis. The phytochemicals contained in *Stachys* act as bio-reductant of $Cu^{2+}$ ions and also a stabilizer of $Cu^0$ NP. Under heating conditions in air the $Cu^0$ NP further gets oxidized to furnish biomolecule fabricated CuO NP. The as synthesized CuO nanocatalyst was thoroughly characterized over a wide range of physicochemical techniques. Towards its catalytic applications, the CuO/*S. lavandulifolia* nanocomposite proved its outstanding efficiency in the C–heteroatom

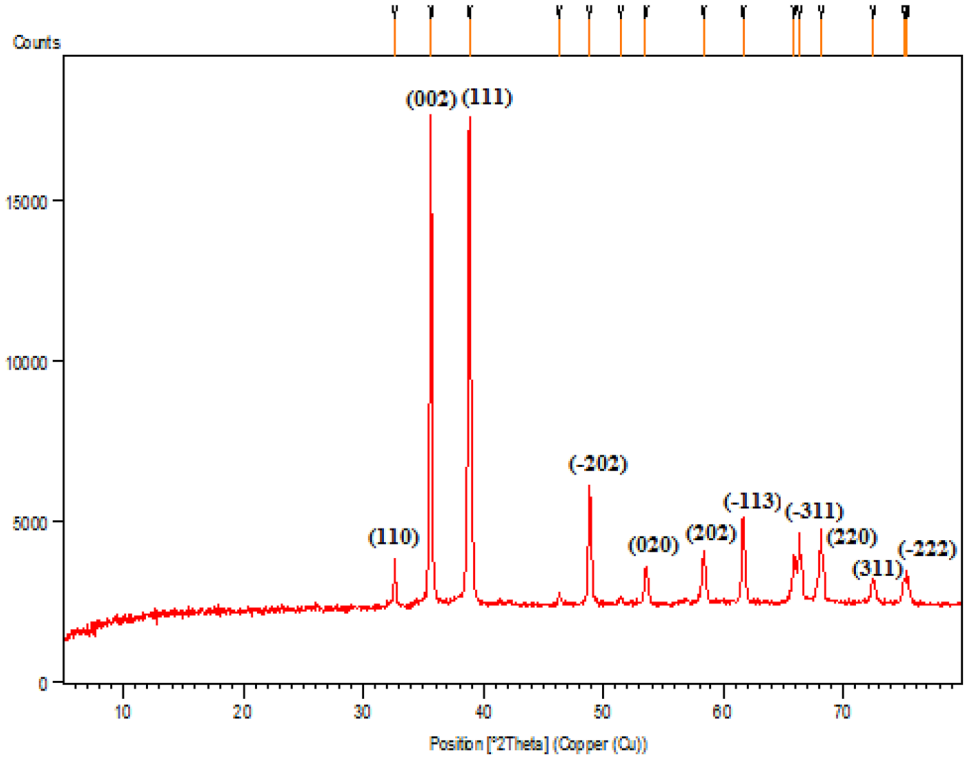


**Figure 8.** Powder XRD pattern of biogenic CuO NPs.

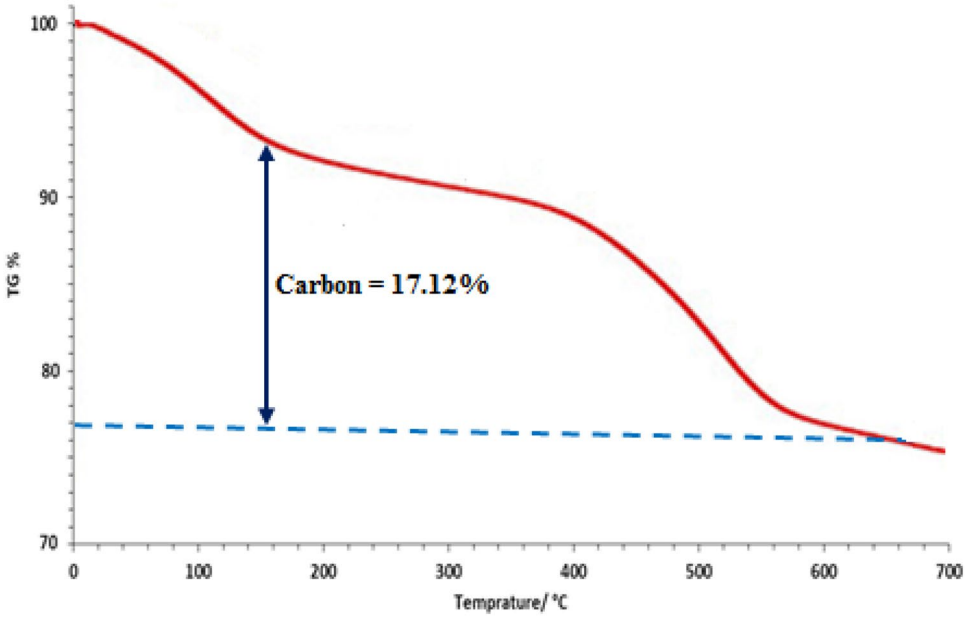


**Figure 9.** TGA profile of CuO NPs.

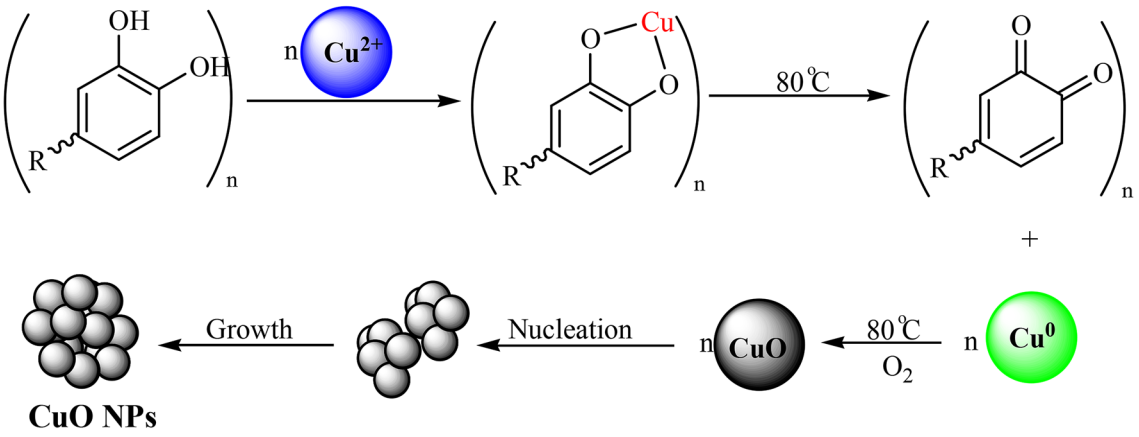


**Scheme 2.** Mechanistic study for the biogenesis of CuO NPs over *Stachys lavandulifolia* extract.

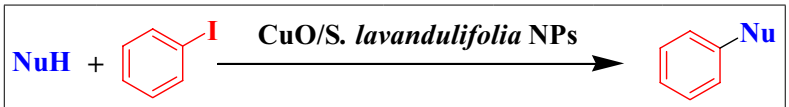


| Entry | NuH | Cat. (mol%) | Base | Solvent | t (h) | Yield (%)[b] |
|---|---|---|---|---|---|---|
| 1 | Indole | 1 | KOH | EtOH | 12 | 60 |
| 2 | Indole | 1 | KOH | DMSO | 10 | 78[c] |
| 3 | Indole | 1 | KOH | Toluene | 12 | 70 |
| 4 | Indole | 1 | KOH | DMF | 12 | 70 |
| 5 | Indole | 1 | KOH | $CH_2Cl_2$ | 24 | 45 |
| 6 | Indole | 1 | KOH | $CH_3CN$ | 24 | 55 |
| 7 | Indole | 2 | KOH | DMSO | 10 | 88[c] |
| 8 | Indole | 3 | KOH | DMSO | 10 | 95[c] |
| 9 | Indole | 3 | - | DMSO | 24 | Trace[c] |
| 10 | Indole | - | KOH | DMSO | 24 | 0[c] |
| 11 | Indole | 3 | $K_2CO_3$ | DMSO | 10 | 70[c] |
| 12 | Indole | 3 | $Na_2CO_3$ | DMSO | 10 | 60[c] |
| 13 | Indole | 3 | $Et_3N$ | DMSO | 10 | 80[c] |
| 14 | Indole | 3 | $NaHCO_3$ | DMSO | 10 | 65[c] |
| 15 | Indole | 3 | KOH | DMSO | 10 | 60[d] |
| 16 | Indole | 3 | KOH | DMSO | 10 | 35[e] |
| 17 | Phenol | 3 | KOH | DMSO | 8 | 92f. |
| 18 | Benzenethiol | 3 | KOH | DMSO | 7 | 96[g] |

**Table 1.** Optimization of reaction condition for CuO/*S. lavandulifolia* NPs -catalyzed coupling of indole/phenol/benzenethiol with iodobenzene. Reaction conditions: N/O/S nucleophile (1.0 mmol), iodobenzene (1.1 mmol), CuO/*S. lavandulifolia* NPs, base (1.5 mmol), solvent (3.0 mL),$N_2$ atmosphere; [b]Isolated yield; [c]100 °C; [d]70 °C; [e]25 °C.

coupling reactions of aryl and heteroaryl nucleophiles with substituted aryl iodides. The approach is effectively deployed towards diverse indole, imidazole, aniline, phenol and thiophenol derivatives in excellent yields. Hitherto known, this is the first report representative of biosynthesized CuO/*Stachys lavandulifolia* NP catalyzed C–heteroatom coupling reaction. The green protocol draws attention in terms of its simple, handy and cost-effective biogenesis of nanocatalyst, convenient operations, recyclability of catalyst and exceptional productivity.

| Entry | Substrate | Aryl iodide | Time (h) | Yield (%)[b] | Ref[c] | TOF ($h^{-1}$)[d] |
|---|---|---|---|---|---|---|
| 1 | Indole | $C_6H_5I$ | 10 | 95 | [65] | 3.16 |
| 2 | Indole | *p*-$CH_3C_6H_4I$ | 11 | 90 | [76] | 2.72 |
| 3 | Indole | *p*-$ClC_6H_4I$ | 10 | 95 | [65] | 3.16 |
| 4 | Indole | *p*-$CH_3OC_6H_4I$ | 12 | 92 | [65] | 2.55 |
| 5 | Indole | *p*-$NO_2C_6H_4I$ | 9 | 96 | [65] | 3.55 |
| 6 | Indole | *o*-$CH_3OC_6H_4I$ | 12 | 90 | [65] | 2.50 |
| 7 | Aniline | $C_6H_5I$ | 4 | 96 | [66] | 8.00 |
| 8 | Aniline | *p*-$CH_3C_6H_4I$ | 4 | 95 | [67] | 7.91 |
| 9 | Aniline | *p*-$ClC_6H_4I$ | 4 | 90 | [67] | 7.5 |
| 10 | Aniline | *p*-$CH_3OC_6H_4I$ | 5 | 90 | [70] | 6.00 |
| 11 | Aniline | *p*-$NO_2C_6H_4I$ | 3 | 96 | [66] | 10.00 |
| 12 | Aniline | *o*-$CH_3OC_6H_4I$ | 2 | 88 | [71] | 14.66 |
| 13 | Imidazole | $C_6H_5I$ | 12 | 90 | [67] | 2.50 |
| 14 | Imidazole | *p*-$CH_3C_6H_4I$ | 12 | 85 | [74] | 2.36 |
| 15 | Imidazole | *p*-$CH_3OC_6H_4I$ | 10 | 75 | [75] | 2.50 |
| 16 | Phenol | $C_6H_5I$ | 8 | 92 | [77] | 3.83 |
| 17 | Phenol | *p*-$CH_3C_6H_4I$ | 9 | 90 | [69] | 3.33 |
| 18 | Phenol | *p*-$ClC_6H_4I$ | 8 | 90 | [71] | 3.75 |
| 19 | Phenol | *p*-$CH_3OC_6H_4I$ | 9 | 92 | [71] | 3.40 |
| 20 | Phenol | *p*-$NO_2C_6H_4I$ | 7 | 96 | [71] | 4.57 |
| 21 | Phenol | *o*-$CH_3OC_6H_4I$ | 12 | 80 | [68] | 2.22 |
| 22 | 4-Methylphenol | $C_6H_5I$ | 12 | 85 | [73] | 2.36 |
| 23 | 4-Methoxylphenol | $C_6H_5I$ | 10 | 96 | [68] | 3.20 |
| 24 | 2-Methylphenol | $C_6H_5I$ | 15 | 90 | [68] | 2.00 |
| 25 | Benzenethiol | $C_6H_5I$ | 7 | 96 | [71] | 4.57 |
| 26 | Benzenethiol | *p*-$CH_3C_6H_4I$ | 8 | 90 | [71] | 3.75 |
| 27 | Benzenethiol | *p*-$ClC_6H_4I$ | 8 | 95 | [71] | 3.95 |
| 28 | Benzenethiol | *p*-$CH_3OC_6H_4I$ | 9 | 90 | [71] | 3.33 |
| 29 | Benzenethiol | *p*-$NO_2C_6H_4I$ | 6 | 98 | [71] | 5.44 |
| 30 | Benzenethiol | *o*-$CH_3OC_6H_4I$ | 10 | 85 | [71] | 2.83 |
| 31 | 4-Methylbenzenethiol | $C_6H_5I$ | 9 | 95 | [72] | 3.51 |
| 32 | 4-Methoxylbenzenethiol | $C_6H_5I$ | 6 | 98 | [72] | 5.44 |

**Table 2.** CuO/*S. lavandulifolia* NPs -catalyzed coupling of amines, phenols, and thiols with aryl iodides. Reaction conditions: amines/phenols/thiols (1.0 mmol), iodobenzene (1.1 mmol), catalyst (3 mol%), KOH (1.5 mmol), stirring in DMSO (3.0 mL) in $N_2$ at 100 °C; [b]Isolated yield; [c]Known product; [d]TOF, turnover frequencies (TOF = (Yield/Time)/Amount of catalyst (mol).

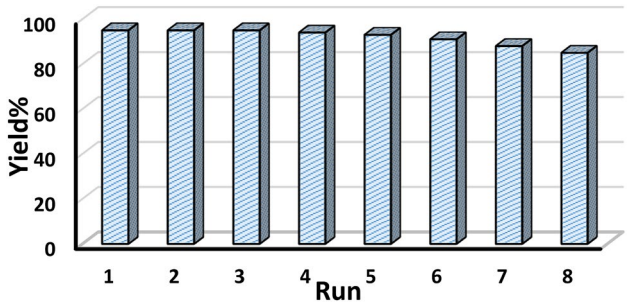


**Figure 10.** Reusable nature of the catalyst.

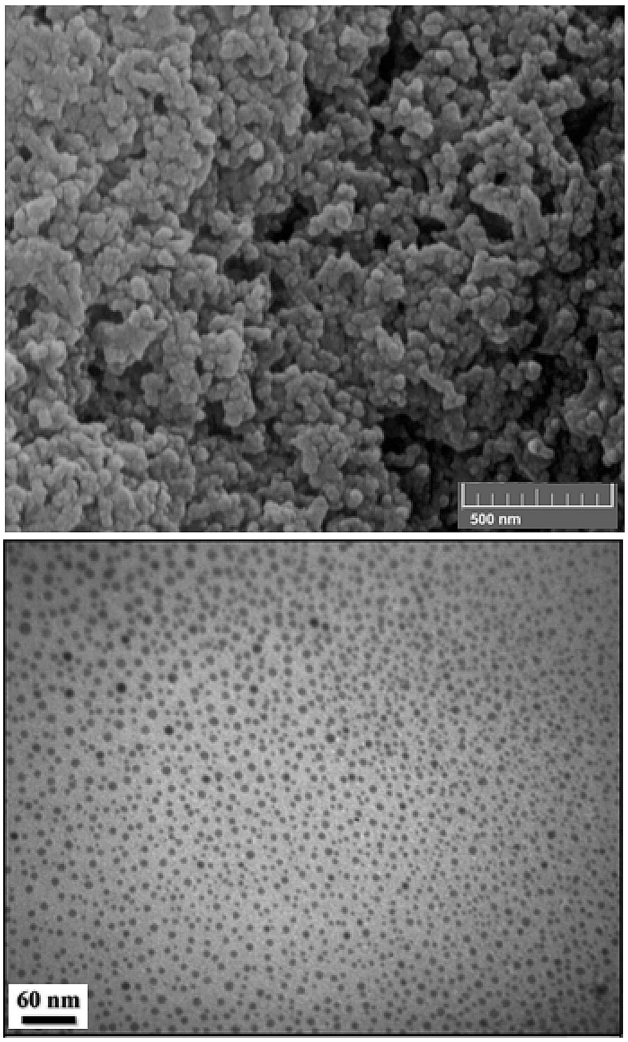


**Figure 11.** FESEM and TEM images of 7 time reused catalyst.

Received: 30 July 2020; Accepted: 4 January 2021
Published online: 21 January 2021

## References

1. Antonyraj, C. A. *et al.* Selective oxidation of HMF to DFF using Ru/γ-alumina catalyst in moderate boiling solvents toward industrial production. *J. Ind. Eng. Chem.* **19**(3), 1056–1059 (2013).
2. Neville, F., Pchelintsev, N. A., Broderick, M. J. F., Gibson, T. & Millner, P. A. Novel one-pot synthesis and characterization of bioactive thiol-silicate nanoparticles for biocatalytic and biosensor applications. *Nanotechnology* **20**(5), 055612 (2009).
3. Menon, S., Rajeshkumar, S. & Venkatkumar, S. A review on biogenic synthesis of gold nanoparticles, characterization, and its applications. *Resour. Eff. Technol.* **3**, 516–527 (2017).
4. Emmanuel, R. *et al.* Antimicrobial efficacy of drug blended biosynthesized colloidal gold nanoparticles from *Justiciaglauca* against oral pathogens: A nanoantibiotic approach. *Microb. Pathog.* **113**, 295–302 (2017).
5. Saravanan, M., Jacob, V., Arockiaraj, J. & Prakash, P. Extracellular biosynthesis, characterization and antibacterial activity of silver nanoparticles synthesized by *Bacillus subtilis* (NCIM-2266). *J. Bionanosci.* **8**(1), 21–27 (2014).
6. Saravanan, M. *et al.* Nano-medicine as a newly emerging approach to combat human immunodeficiency virus (HIV). *Pharm. Nanotechnol.* **6**(1), 17–27 (2018).
7. Saravanan, M., Hamed, B., Balajee, R., Gopinath, V. & Karuppiah, P. Chapter eleven-emerging plant-based anti-cancer green nanomaterials in present scenario. *Comp. Anal. Chem.* **87**, 291–318 (2019).
8. Barabadi, H. *et al.* Emerging theranostic silver and gold nanomaterials to combat prostate cancer: a systematic review. *J. Clust. Sci.* **30**, 1375–1382 (2019).
9. Barabadi, H. *et al.* Penicillium family as emerging nanofactory for biosynthesis of green nanomaterials: A journey into the world of microorganisms. *J. Clust. Sci.* **30**, 843–856 (2019).
10. Roy, N., Gaur, A., Jain, A., Bhattacharya, S. & Rani, V. Green synthesis of silver nanoparticles: An approach to overcome toxicity. *Environ. Toxicol. Pharmacol.* **36**(3), 807–812 (2013).
11. Xia, Y., Yang, H. & Campbell, C. T. Nanoparticles for catalysis. *Acc. Chem. Res.* **46**(8), 1671–1672 (2013).
12. Nemati, M., Tamoradi, T. & Veisi, H. Immobilization of Gd(III) complex on $Fe_3O_4$: A novel and recyclable catalyst for synthesis of tetrazole and S–S coupling. *Polyhedron* **167**, 75–84 (2019).

13. Veisi, H., Taheri, S. & Hemmati, S. Preparation of polydopamine sulfamic acid-functionalized magnetic $Fe_3O_4$ nanoparticles with a core/shell nanostructure as heterogeneous and recyclable nanocatalysts for the acetylation of alcohols, phenols, amines and thiols under solvent-free conditions. *Green Chem.* **18**, 6337–6348 (2016).
14. Ghorbani, R. H., Safekordi, A. A., Attar, H. & Sorkhabadi, R. S. M. Biological and non-biological methods for silver nanoparticles synthesis. *Chem. Biochem. Eng. Q.* **25**, 317–326 (2011).
15. Duan, H., Wang, D. & Li, Y. Green chemistry for nanoparticle synthesis. *Chem. Soc. Rev.* **44**, 5778–5792 (2015).
16. Dewan, A., Sarmah, M., Thakur, A. J., Bharali, P. & Bora, U. Greener biogenic approach for the synthesis of palladium nanoparticles using papaya peel: An eco-friendly catalyst for C–C coupling reaction. *ACS Omega* **3**, 5327–5335 (2018).
17. Xu, H.-J. *et al.* CuI-nanoparticles-catalyzed selective synthesis of phenols, anilines, and thiophenols from aryl halides in aqueous solution. *J. Org. Chem.* **76**, 2296–2300 (2011).
18. Ingale, A. G. & Chaudhari, A. N. Biogenic synthesis of nanoparticles and potential applications: An ecofriendly approach. *J. Nanomed. Nanotechnol.* **4**, 165 (2013).
19. Vishnukumar, P., Vivekanandhan, S. & Muthuramkumar, S. Plant-mediated biogenic synthesis of palladium nanoparticles: Recent trends and emerging opportunities. *Plant ChemBioEng Rev.* **4**, 18–36 (2017).
20. Mittal, A. K., Chisti, Y. & Banerjee, U. C. Synthesis of metallic nanoparticles using plant extracts. *Biotechnol. Adv.* **31**, 346–356 (2013).
21. Anandan, M. *et al.* Green synthesis of anisotropic silver nanoparticles from the aqueous leaf extract of *Dodonaeaviscosa* with their antibacterial and anticancer activities. *Process Biochem.* **80**, 80–88 (2019).
22. Ovais, M. *et al.* Role of plant phytochemicals and microbial enzymes in biosynthesis of metallic nanoparticles. *Appl. Microbiol. Biotechnol.* **102**, 6799–6814 (2018).
23. Saravanan, M. *et al.* Green synthesis of anisotropic zinc oxide nanoparticles with antibacterial and cytofriendly properties. *Microb. Pathog.* **115**, 57–63 (2018).
24. Padil, V. V. T. & Cerník, M. Green synthesis of copper oxide nanoparticles using gum karaya as a biotemplate and their antibacterial application. *Int. J. Nanomed.* **8**, 889–898 (2013).
25. Abboud, Y. *et al.* Biosynthesis, characterization and antimicrobial activity of copper oxide nanoparticles (CONPs) produced using brown alga extract (*Bifurcaria bifurcata*). *Appl. Nanosci.* **4**, 571–576 (2014).
26. Xiong, J., Wang, Y., Xue, Q. & Wu, X. Synthesis of highly stable dispersions of nanosized copper particles using L-ascorbic acid. *Green Chem.* **13**, 900–904 (2011).
27. Ko, Y. L., Krishnamurthy, S. & Yun, Y. S. Facile synthesis of monodisperse Pt and Pd nanoparticles using antioxidants. *J. Nanosci. Nanotechnol.* **15**, 412–417 (2015).
28. Kharissova, O. V., Dias, H. V. R., Kharisov, B. I., Pérez, B. O. & Pérez, V. M. The greener synthesis of nanoparticles. *Trends Biotechnol.* **31**, 240–248 (2013).
29. Shankar, S. S., Rai, A., Ahmad, A. & Sastry, M. Rapid synthesis of Au, Ag, and bimetallic Au core–Ag shell nanoparticles using Neem (*Azadirachta indica*) leaf broth. *J. Colloid Interface Sci.* **275**, 496–502 (2004).
30. Sarmah, M. *et al.* Effect of substrates on catalytic activity of biogenic palladium nanoparticles in C–C cross-coupling reactions. *ACS Omega* **4**, 3329–5340 (2019).
31. Veisi, H., Ghorbani, M. & Hemmati, S. Sonochemical *in situ* immobilization of Pd nanoparticles on green tea extract coated $Fe_3O_4$ nanoparticles: An efficient and magnetically recyclable nanocatalyst for synthesis of biphenyl compounds under ultrasound irradiations. *Mater. Sci. Eng. C.* **98**, 584–593 (2019).
32. Shahriary, M., Veisi, H., Hekmati, M. & Hemmati, S. In situ green synthesis of Ag nanoparticles on herbal tea extract (*Stachys lavandulifolia*)-modified magnetic iron oxide nanoparticles as antibacterial agent and their 4-nitrophenol catalytic reduction activity. *Mater. Sci. Eng. C* **90**, 57–66 (2018).
33. Kamal, A. *et al.* Water mediated Heck and Ullmann couplings by supported palladium nanoparticles: importance of surface polarity of the carbon spheres. *Green Chem.* **14**, 2513–2522 (2012).
34. He, L. *et al.* In situ synthesis of gold nanoparticles/metal–organic gels hybrids with excellent peroxidase-like activity for sensitive chemiluminescence detection of organophosphorus pesticides. *ACS Appl. Mater. Interfaces* **10**, 28868–28876 (2018).
35. Gaikwad, A. V. & Rout, T. K. *In situ* synthesis of silver nanoparticles in polyetherimide matrix and its application in coatings. *J. Mater. Chem.* **21**, 1234–1239 (2011).
36. Hartwig, J. F. Transition metal catalyzed synthesis of arylamines and aryl ethers from aryl halides and triflates: Scope and mechanism. *Angew. Chem. Int. Ed.* **37**, 2046–2067 (1998).
37. Anilkumar, K., Kannaboina, P. & Das, P. Ruthenium-catalyzed site-selective C–H arylation of 2-pyridones and 1-isoquinolinones. *Org. Biomol. Chem.* **15**, 5757–5461 (2017).
38. Bera, M. *et al.* Rhodium-catalyzed *meta*-C–H functionalization of arenes. *Angew. Chem. Int. Ed.* **56**(19), 5272–5276 (2017).
39. Kumar, S., Kumar, P., Deb, A., Maity, D. & Jain, S. L. Graphene oxide grafted with iridium complex as a superior heterogeneous catalyst for chemical fixation of carbon dioxide to dimethylformamide. *Carbon* **100**, 632–640 (2016).
40. Kuo, C.-H. & Huang, M. H. Morphologically controlled synthesis of $Cu_2O$ nanocrystals and their properties. *Nano Today.* **5**, 106–116 (2010).
41. Zhang, Q. *et al.* CuO nanostructures: Synthesis, characterization, growth mechanisms, fundamental properties, and applications. *Prog. Mater. Sci.* **60**, 208–337 (2014).
42. Wang, X. & Xu, X. Thermal conductivity of nanoparticle-fluid mixture. *J. Thermophys. Heat Transf.* **13**(4), 474–480 (1999).
43. Xu, J. *et al.* Synthesis of Au and Pt hollow capsules with single holes via pickering emulsion strategy. *J. Phys. Chem. C* **119**, 28055–28060 (2015).
44. Xu, J. *et al.* Hierarchical CuO colloidosomes and their structure enhanced photothermal catalytic activity. *J. Phys. Chem. C* **120**, 12666–12672 (2016).
45. Das, V. K., Borah, M. & Thakur, A. J. Piper-betle-shaped nano-S-catalyzed synthesis of 1-amidoalkyl-2-naphthols under solvent-free reaction condition: A Greener, "Nanoparticle-Catalyzed Organic Synthesis Enhancement" approach. *J. Org. Chem.* **78**, 3361–3366 (2013).
46. Das, V. K., Devi, R. R., Raul, P. K. & Thakur, A. J. Nano rod-shaped and reusable basic $Al_2O_3$catalyst for *N*-formylation of amines under solvent-free conditions: A novel, practical and convenient 'NOSE' approach. *Green Chem.* **14**, 847–854 (2012).
47. Evano, G., Blanchard, N. & Toumi, M. Copper-mediated coupling reactions and their applications in natural products and designed biomolecules synthesis. *Chem. Rev.* **108**, 3054 (2008).
48. Corbet, J. P. & Mignani, G. selected patented cross-coupling reaction technologies. *Chem. Rev.* **106**, 2651 (2006).
49. Luza, L., Gual, A. & Dupont, J. The partial hydrogenation of 1,3-dienes catalysed by soluble transition-metal nanoparticles. *ChemCatChem* **6**, 702–710 (2014).
50. Meijere, A. & Diederich, F. (eds) *Metal-Catalyzed Cross-Coupling Reactions* (Wiley, Weinheim, 2004).
51. Weingarten, H. Mechanism of the Ullmann condensation. *J. Org. Chem.* **29**, 3624–3626 (1964).
52. Antilla, J. C., Klapars, A. & Buchwald, S. L. The Copper-catalyzed *N*-arylation of indoles. *J. Am. Chem. Soc.* **124**, 11684–11688 (2002).
53. Toummini, D., Tlili, A., Berges, J., Ouazanni, F. & Taillefer, M. Copper-catalyzed arylation of nitrogen heterocycles from anilines under ligand-free conditions. *Chem. Eur. J.* **20**, 14619–14623 (2014).

54. Monnier, F. & Taillefer, M. Catalytic C–C, C–N, and C–O Ullmann-type coupling reactions: Copper makes a difference. *Angew. Chem. Int. Ed.* **47**, 3096–3099 (2008).
55. Monnier, F. & Taillefer, M. Catalytic C–C, C–N, and C–O Ullmann-type coupling reactions. *Angew. Chem. Int. Ed.* **48**, 6954–6971 (2009).
56. Bhunia, S., Pawar, G. G., Vijay Kumar, S., Jiang, Y. & Ma, D. Selected copper-based reactions for C–N, C–O, C–S, and C–C bond formation. *Angew. Chem. Int. Ed.* **56**, 16136–16179 (2017).
57. Pradhan, S., De, P. B. & Punniyamurthy, T. Copper(II)-mediated chelation-assisted regioselective *N*-naphthylation of indoles, pyrazoles and pyrrole through dehydrogenative cross-coupling. *J. Org. Chem.* **82**, 4883–4890 (2017).
58. Mahesh, D., Sadhu, P. & Punniyamurthy, T. Copper(II)-catalyzed oxidative cross-coupling of anilines, primary alkyl amines, and sodium azide using TBHP: A route to 2-substituted benzimidazoles. *J. Org. Chem.* **81**, 3227–3234 (2016).
59. Veisi, H., Rashtiani, A. & Barjasteh, V. Biosynthesis of palladium nanoparticles using *Rosa canina* fruit extract and their use as a heterogeneous and recyclable catalyst for Suzuki–Miyaura coupling reactions in water. *Appl. Organometal. Chem.* **30**, 231–235 (2016).
60. Veisi, V., Hemmati, S. & Shirvani, H. Green synthesis and characterization of monodispersed silver nanoparticles obtained using oak fruit bark extract and their antibacterial activity. *Appl. Organometal. Chem.* **30**, 387–391 (2016).
61. Nagajyothi, P. C., Muthuraman, P., Sreekanth, T. V. M., Kim, D. H. & Shim, J. Green synthesis: *In-vitro* anticancer activity of copper oxide nanoparticles against human cervical carcinoma cells. *Arab. J. Chem.* **10**, 215–225 (2017).
62. Kumar, V. *et al.* Photo-mediated optimized synthesis of silver nanoparticles for the selective detection of Iron(III), antibacterial and antioxidant activity. *Mater. Sci. Eng. C.* **71**, 1004–1019 (2017).
63. Dorman, H. J. D. & Deans, S. G. Antimicrobial agents from plants: Antibacterial activity of plant volatile oils. *J. Appl. Microbiol.* **88**, 308–316 (2000).
64. Nasrollahzadeh, M., Maham, M. & Sajadi, S. M. Green synthesis of CuO nanoparticles by aqueous extract of *Gundelia tournefortii* and evaluation of their catalytic activity for the synthesis of *N*-monosubstituted ureas and reduction of 4-nitrophenol. *J. Colloid. Interference Sci.* **455**, 245–253 (2015).
65. Xie, Y. X., Pi, S. F., Wang, J., Yin, D. L. & Li, J. H. 2-Aminopyrimidine-4,6-diol as an efficient ligand for solvent-free copper-catalyzed *N*-Arylations of imidazoles with aryl and heteroaryl halides. *J. Org. Chem.* **71**, 8324–8327 (2006).
66. Huang, Y. Z., Gao, J., Ma, H., Miao, H. & Xu, J. Ninhydrin: An efficient ligand for the Cu-catalyzed *N*-arylation of nitrogen-containing heterocycles with aryl halides. *Tetrahedron Lett.* **49**, 948–951 (2008).
67. Kantam, M. L., Roy, R., Roy, S., Sreedhar, B. & De, R. L. Polyaniline supported CuI: An efficient catalyst for C–N bond formation by *N*-arylation of *N*(H)-heterocycles and benzyl amines with aryl halides and arylboronic acids, and aza-Michael reactions of amines with activated alkenes. *Catal. Commun.* **9**, 2226–2230 (2008).
68. Islam, S. M. *et al.* A reusable polymer supported copper catalyst for the C–N and C–O bond cross-coupling reaction of aryl halides as well as arylboronic acids. *J. Organomet. Chem.* **696**, 4264–4274 (2012).
69. Tao, M. & Lei, W. Immobilization of copper in organic–inorganic hybrid materials: A highly efficient and reusable catalyst for the Ullmann diaryl etherification. *Tetrahedron Lett.* **48**, 95–99 (2007).
70. Jogdand, N. R., Shingate, B. B. & Shingare, M. S. Tris-(2-aminoethyl) amine as a novel and efficient tripod ligand for a copper(I)-catalyzed C-O coupling reaction. *Tetrahedron Lett.* **50**, 4019–4021 (2009).
71. Jammi, S. *et al.* CuO nanoparticles catalyzed C–N, C–O, and C–S cross-coupling reactions: Scope and mechanism. *J. Org. Chem.* **74**, 1971–1976 (2009).
72. Rout, L., Sen, T. K. & Punniyamurthy, T. Efficient CuO-nanoparticle-catalyzed C–S cross-coupling of thiols with iodobenzene. *Angew. Chem. Int. Ed.* **46**, 5583 (2007).
73. Veisi, H., Hamelian, M., Hemmati, S. & Dalvand, A. CuI catalyst heterogenized on melamine-pyridines immobilized SBA-15: Heterogeneous and recyclable nanocatalyst for Ullmann-type C–N coupling reactions. *Tetrahedrom Lett.* **58**, 4440–4446 (2017).
74. Ghorbani-Vaghei, R., Hemmati, S. & Veisi, H. An in situ generated CuI/metformin complex as a novel and efficient catalyst for C–N and C–O cross-coupling reactions. *Tetrahedron Lett.* **54**, 7095–7099 (2013).
75. Zhu, J. B., Cheng, L., Zhang, Y., Xie, R. G. & You, J. S. highly efficient copper-catalyzed *N*-arylation of nitrogen-containing heterocycles with aryl and heteroaryl halides. *J. Org. Chem.* **72**, 2737–2743 (2007).
76. Veisi, H., Metghalchi, Y., Hekmati, M. & Samadzadeh, S. CuI heterogenized on thiosemicarbazide modified-multi walled carbon nanotubes (thiosemicarbazide-MWCNTs-CuI): Novel heterogeneous and reusable nanocatalyst in the C–N Ullmann coupling reactions. *Appl. Organomet. Chem.* **31**, 3676 (2017).
77. Akhavan, M., Hemmati, S., Hekmati, M. & Veisi, H. CuCl heterogenized on metformine-modified multi walled carbon nanotubes as a recyclable nanocatalyst for Ullmann-type C-O and C–N coupling reactions. *New J. Chem.* **42**, 2782–2789 (2018).


## Acknowledgements

We express gratitude to Payame Noor University (PNU) for financial supports. BK thanks Gobardanga Hindu College for affiliations.

## Author contributions

T.T., B.K., S.H., M.H. and M.H. wrote the main manuscript and H.V. prepared figures. All authors reviewed the manuscript.

## Competing interests

The authors declare no competing interests.

## Additional information

**Correspondence** and requests for materials should be addressed to H.V. or B.K.

**Reprints and permissions information** is available at www.nature.com/reprints.

**Publisher's note** Springer Nature remains neutral with regard to jurisdictional claims in published maps and institutional affiliations.